Applied Catalysis B: Environmental 97 (2010) 127–134

Contents lists available at ScienceDirect

Applied Catalysis B: Environmental

journal homepage: www.elsevier.com/locate/apcatb

Catalytic wet air oxidation of phenol with air and micellar molybdovanadophosphoric polyoxometalates under room condition

Shun Zhao [a], Xiaohong Wang [a,*], Mingxin Huo [b,*]

[a] Key Lab of Polyoxometalate Science of Ministry of Education, Faculty of Chemistry, Northeast Normal University, 5268 Renmin Street, Changchun 130024, Jilin Province, PR China
[b] School of Urban and Environmental Sciences, Northeast Normal University, Changchun 130024, PR China

ARTICLE INFO

Article history:
Received 11 November 2009
Received in revised form 23 March 2010
Accepted 24 March 2010
Available online 31 March 2010

Keywords:
Catalytic wet air oxidation
Polyoxometalate
Micellar catalysis
Degradation of phenol

ABSTRACT

Micellar molybdovanadophosphoric polyoxometalate (POM) catalysts $[(C_nH_{2n+1})N(CH_3)_3]_{3+x}PV_xMo_{12-x}O_{40}$ ($x = 1, 2, 3$; $n = 8, 12, 14, 16, 18$) were prepared and used for catalytic wet air oxidation (CWAO) of phenol. X-ray photoelectron spectrum (XPS), Fourier transform infrared spectroscopy (FT-IR), transmission electron microscopy (TEM) were used to characterize the resulting samples. The best catalytic activity was obtained over $(C_{16}TA)_6PV_3Mo_9O_{40}$, which showed 95.3% degradation efficiency, 98.5% COD removal and 93.0% TOC reduction with air under room condition toward complete degradation product CO_2 within 90 min. The leaching test showed that the POM micellar catalysts have an excellent stability and can be used as heterogeneous catalysts for about six times.

1. Introduction

The wet air oxidation (WAO), a treatment firstly patented over 50 years ago [1], uses oxygen or air to oxidize organic compounds completely into carbon dioxide and water [2]. It is a clean process that does not involve any harmful chemical reagent. However, a non-catalytic process requires high temperatures and high pressures to achieve complete oxidation, resulting in high operating costs which limit practical applications. Catalytic wet air oxidation (CWAO) strongly improves the degradation of organic pollutants under milder conditions of temperature and pressure conditions. It is an effective process for treating highly concentrated organic wastewater [2]. Heterogeneous catalysts are more desirable because homogeneous catalysts require an additional separation step for the soluble species [3] leading to high treatment costs. Transition metal oxides (e.g., Cu, Fe, Co, Mn, Ni, Sn, and many other oxides in various combinations) and supported noble metals (e.g., Pt, Pd, Ru, and Rh) have been applied in CWAO. Noble metal catalysts have been proven to be efficient for the CWAO of a wide range of pollutants, including carboxylic acids [4–7], phenol [8–16], and nitrogen compounds [17,18]. These two techniques have three main drawbacks. One is the high cost of noble metals and their high installation cost. Second is the possibly incomplete oxidation of phenol to CO_2 by metal oxides. A range of organic compounds formed as intermediates or byproducts during the mineralization process, some of which are more toxic than the original pollutants. Third, the leaching of most transition metal oxides results in solid catalyst deactivation. Thus, the lack of active and durable catalysts under mild condition has prevented CWAO from being implemented for environmental remediation [19].

Polyoxometalates (POMs) also named heteropolyacids (HPAs) are oxo-clusters of early transition metals in their highest oxidation states, namely Mo (VI), W (VI) or V (V). They represent an increasingly important class of environmentally benign catalysts that can be used even under rather mild conditions for the oxidation of a number of organic substrates in the presence of either molecular oxygen or other donors [20]. Among POMs, the Keggin-type molybdovanadophosphoric acids, $H_{3+x}PV_xMo_{12-x}O_{40}$ ($x = 1$–6), have been found widely used in the selective oxidation of different organic compounds with O_2 [21–23]. Earlier research showed that molybdovanadophosphates could catalyze organic reactions through the electron-transfer oxidation of a substrate by POMs, which could be reoxidized by oxygen [21]. Birchmeier et al. [24] had employed $Na_5PV_2Mo_{10}O_{40}$ (0.05 M) to treat phenol (5.4 mM) in the CWAO process under a mild reaction condition (155 °C and 0.93 MPa of oxygen pressure), and found that high COD removals (76%) can be achieved over 1 h. However, this homogeneous system has limited industrial applications due to the difficulty of separation and recovery of the catalyst. To date, there are no reports on CWAO of phenol under extremely mild condition such as ambient temperature and atmospheric pressure.

The utilization of surfactants to form micelles is most often used to significantly accelerate the reaction rate in a micellar

* Corresponding authors. Tel.: +86 431 88930042; fax: +86 431 85099759.
E-mail addresses: wangxh665@nenu.edu.cn, wxh.wangxiaohong665@yahoo.com.cn (X. Wang).

0926-3373/$ – see front matter © 2010 Elsevier B.V. All rights reserved.
doi:10.1016/j.apcatb.2010.03.032

medium [25]. Amphiphilic quaternary ammonium micelles such as cetyltrimethyl ammonium bromide (CTAB) micelles are very useful in trapping environmental contaminants and have been applied in environmental remediation. CTAB micelles are considered viable in the micellar enhanced ultrafiltration process because they are very effective in dissolving phenols [26]. Amphiphilic quaternary ammonium micelles of POMs with a surfactant core and a POM surface can form supramolecular micellar assemblies ranging from nanoscale to microscale sizes in aqueous solutions. This structure could possibly afford high local reactant concentrations near the catalysts, helping to overcome the limited solubility of hydrophobic substrates in water. Amphiphilic POM catalysts have been successfully used in various organic synthesis reactions with hydrogen peroxide [27–32] as an oxidant in an emulsion or microemulsion system. Using molecular oxygen instead of hydrogen peroxide as an oxidant has long been desired due to its lower cost and green chemistry advantages. Thus far, only Li [33] has reported on the oxidative desulfurization of dibenzothiophene with O_2 using amphiphilic POM emulsion catalysts. Few studies have been conducted to develop amphiphilic POM micellar catalysts for a direct degradation of organic pollutants in the CWAO process.

Previous work in our laboratory [34,35], as well as other studies [36], was focused on investigating heterogeneous POM catalysts in CWAO. Compared to the quick development of POM-based photocatalysts for pollutant removal [37], few studies have reported on the use of POMs in the CWAO of organic pollutants. Hence, the search for a more active and stable heterogeneous POM catalyst to lower the oxidation condition requirements for WAO is an ongoing challenge.

In this paper, we focus on POM micellar catalysts $[(C_nH_{2n+1})N(CH_3)_3]_{3+x}PV_xMo_{12-x}O_{40}$ (x = 1, 2, 3; n = 8–18) for the CWAO of phenol with air under room temperature and atmospheric pressure. The best catalytic activity was obtained over $(C_{16}TA)_6PV_3Mo_9O_{40}$ in air under room conditions. This resulted to 95.3% degradation of 0.72 mM phenol and the evolution of the complete degradation product CO_2 within a short time. The leaching test showed that $(C_{16}TA)_6PV_3Mo_9O_{40}$ had an excellent stability and could be reused about six times as a rapid heterogeneous catalyst by a simple treatment. Herein three main innovations are achieved: (1) activation of O_2 by micellar POM catalysts; (2) first example of a highly efficient degradation of phenol under extremely mild conditions using a micellar POM system; and (3) best results achieved within a short time at ambient temperature and atmospheric pressure for the CWAO of phenol using air as an oxidant.

2. Experimental

2.1. Materials

All reagents were of AR grade and used without further purification. For oxidation degradation, 0.1 M stock solution of phenol was prepared and aqueous solution of needed concentration was prepared from the stock solution. Molybdovanadophosphoric acids were prepared according to Ref. [38], and were characterized by IR spectroscopy.

2.2. Physical measurements

Elemental analysis was carried out using a Leeman Plasma Spec (I) ICP-ES and a P-E 2400 CHN elemental analyzer. FT-IR spectra (4000–400 cm^{-1}) were recorded in KBr discs on a Nicolet Magna 560 IR spectrometer. XPS were recorded on an Escalab-MK II photoelectronic spectrometer with Al K_α (1200 eV). TEM image was measured on JOEL JEM-2100F microscope. Analysis of phenol and intermediates during the reaction was performed by high pressure liquid chromatogram (HPLC, Shimadzu LC-20A) with a UV detector using a Shim-pack VP-ODS (4.6 mm × 250 mm, 5 μm) column. The mobile phase was a mixture of 80% water, and 20% methanol with a flow rate of 1 mL/min. A DX-300 ion chromatograph (IC) equipped with a conductivity detector and an ICE-ASI anion column was also used to determine the changes of the concentrations of the intermediates and final products. Total organic carbon (TOC) was monitored using a Shimadzu TOC-VCPH total organic carbon analysis system. Chemical oxygen demand (COD) was determined by a closed reflux colorimetric method using 756 CRT UV–vis spectrophotometer at a wavelength of 600 nm. The leaching concentrations of $(C_{16}TA)_5PV_2Mo_{10}O_{40}$ during the reaction were also measured through analyzing the dissolved concentration of Mo in aqueous solution using a Leeman Plasma Spec (I) ICP-ES. The cyclic voltammograms were recorded with a CHI660c recorder (China).

2.3. Preparation of $[C_{16}H_{33}N(CH_3)_3]_5PV_2Mo_{10}O_{40}$

10 mL, 200 mM of hexadecyltrimethylammonium bromide (CTAB) aqueous solution was added into 10 mL, 40 mM of $H_5PV_2Mo_{10}O_{40}$ solution with stirring. The white precipitate formed immediately and was collected by filtration, then was calcinated at 100 °C for about 3 h. The resulting $[C_{16}H_{33}N(CH_3)_3]_5PV_2Mo_{10}O_{40}$ (denoted as $(C_{16}TA)_5PV_2Mo_{10}O_{40}$) was obtained with yield 50%. IR (1% KBr pellet, 4000–400 cm^{-1}): 1056 cm^{-1} (sh), 945 cm^{-1} (s), 869 cm^{-1} (m), 789 cm^{-1} (m), and 588 cm^{-1} (w).

The other $(C_{16}TA)_{3+x}PV_xMo_{12-x}O_{40}$ (x = 1, 3) catalysts were prepared in the same procedure except using $H_4PVMo_{11}O_{40}$ and $H_6PV_3Mo_9O_{40}$.

The resulting $(C_{16}TA)_6PV_3Mo_9O_{40}$ was obtained with yield 38%. IR (1% KBr pellet, 4000–400 cm^{-1}): 1156 cm^{-1} (m), 1080 cm^{-1} (sh), 934 cm^{-1} (s), 866 cm^{-1} (m), 777 cm^{-1} (m), 697 cm^{-1} (s), and 545 cm^{-1} (w).

The resulting $(C_{16}TA)_4PVMo_{11}O_{40}$ was obtained with yield 53%. IR (1% KBr pellet, 4000–400 cm^{-1}): 1173 cm^{-1} (m), 1062 cm^{-1} (sh), 957 cm^{-1} (s), 881 cm^{-1} (m), 798 cm^{-1} (m), 578 cm^{-1} (w).

The other amphiphilic quaternary ammonium salts of molybdovanadophosphates were prepared in the same procedure except using $[(C_8H_{17})N(CH_3)_3]Br$ (octal trimethylammonium bromide, O_8TAB), $[(C_{12}H_{25})N(CH_3)_3]Br$ (dodecyl trimethylammonium bromide, $D_{12}TAB$), $[(C_{14}H_{29})N(CH_3)_3]Br$ (tetradecyl trimethylammonium bromide, $T_{14}TAB$), $[(C_{18}H_{37})N(CH_3)_3]Br$ (octadecyl trimethylammonium bromide, $O_{18}TAB$).

2.4. Critical micelle concentration (CMC) determination

The CMC of $(C_{16}TA)_5PV_2Mo_{10}O_{40}$ was determined at break points of nearly two straight line portions of the specific conductivity versus concentration plot [39].

2.5. Catalytic procedure

A typical procedure was carried out as follows: 0.92 mM of catalysts (at the CMC of $(C_{16}TA)_5PV_2Mo_{10}O_{40}$) was suspended in a fresh aqueous phenol solution (C_0 = 0.72 mM, 100 mL, pH = 1.7) in three-neck glass flask at ambient temperature (25 °C). The air was inputted into the bottom of the suspension with the flowing rate 0.04 m^3/h. This process uses oxygen dissolved in the aqueous solution as an oxidant directly. Oxygen concentration depends on the oxygen solubility at room temperature and atmospheric pressure. Samples were withdrawn periodically to be measured. After finishing, the catalyst was separated by centrifuge in 10 000 rpm and washed with water for three times to be reused. All experiments were repeated six times.

Table 1
The data of catalysts' elementary analysis.

Catalysts	Elemental analysis (calcd) wt%					
	C	H	N	Mo	V	P
$(C_{16}TA)_4PMo_{11}V_1O_{40}$	32.09 (31.38)	5.43 (5.51)	1.87 (1.93)	37.56 (36.34)	1.36 (1.75)	1.20 (1.15)
$(C_{16}TA)_5PMo_{10}V_2O_{40}$	35.34 (36.27)	6.19 (6.39)	2.34 (2.23)	31.55 (30.54)	4.01 (3.25)	1.03 (0.98)
$(C_{16}TA)_6PMo_9V_3O_{40}$	41.28 (40.47)	7.15 (7.10)	2.44 (2.49)	23.89 (24.56)	4.76 (4.53)	0.98 (0.96)
$(C_{12}TA)_5PMo_{10}V_2O_{40}$	30.54 (31.33)	5.83 (5.92)	2.49 (2.44)	33.29 (33.41)	3.39 (3.55)	1.06 (1.08)
$(C_{14}TA)_5PMo_{10}V_2O_{40}$	34.04 (33.85)	6.19 (6.31)	2.30 (2.32)	30.97 (31.86)	3.47 (3.39)	1.04 (1.03)
$(C_{18}TA)_5PMo_{10}V_2O_{40}$	37.56 (38.23)	6.77 (6.98)	2.21 (2.13)	28.40 (29.15)	3.22 (3.10)	0.91 (0.93)

Table 2
The CMC of $[(C_nH_{2n+1})N(CH_3)_3]_{3+x}PV_xMo_{12-x}O_{40}$ at 25 °C.

Catalysts	CMC (mol/L)
$(C_{16}TA)_4PVMo_{11}O_{40}$	16.3×10^{-4}
$(C_{16}TA)_6PV_3Mo_9O_{40}$	1.8×10^{-4}
$(C_{16}TA)_5PV_2Mo_{10}O_{40}$	9.2×10^{-4}
$(O_8TA)_5PV_2Mo_{10}O_{40}$	35.8×10^{-4}
$(D_{12}TA)_5PV_2Mo_{10}O_{40}$	24.7×10^{-4}
$(T_{14}TA)_5PV_2Mo_{10}O_{40}$	17.4×10^{-4}
$(O_{18}TA)_5PV_2Mo_{10}O_{40}$	1.7×10^{-4}

2.6. Adsorption experiments

Adsorption experiments were carried out to determine the adsorption capacity of catalysts for phenol. In the simultaneous adsorption experiments, 100 mL of 0.72 mM phenol solution and 0.253 g catalysts were loaded in the bottle with flowing nitrogen instead of air. At the predetermined time intervals, samples were taken and the phenol concentrations were analyzed.

3. Results and discussion

3.1. Characterization of micellar catalysts

From the results of the elemental analyses, the Mo, P and V contents in catalysts are listed in Table 1. Compared with the calculated values, the results are satisfactory.

The IR spectra of different vanadium-substituted POMs were investigated. Peaks in the range of 600–1100 cm^{-1} corresponding to Keggin structural vibrations could be easily distinguished. This indicates that $[(C_nH_{2n+1})N(CH_3)_3]_{3+x}PV_xMo_{12-x}O_{40}$ maintains the Keggin structure.

The cyro-TEM image of $(C_{16}TA)_5PV_2Mo_{10}O_{40}$ shows that it can form relatively uniform-sized (about 20 nm) micellar droplets (Fig. 1).

The CMC of $[(C_nH_{2n+1})N(CH_3)_3]_{3+x}PV_xMo_{12-x}O_{40}$ was given in Table 2.

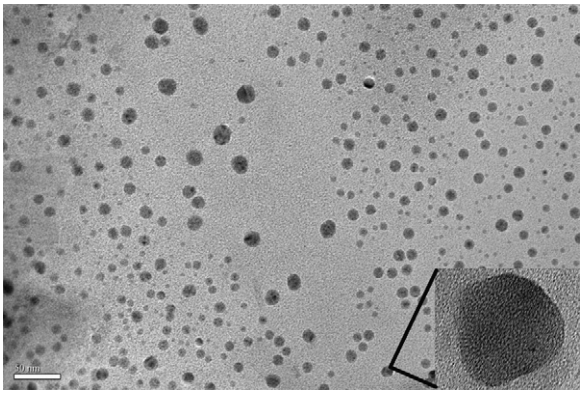

Fig. 1. The cyro-TEM image of $(C_{16}TA)_5PV_2Mo_{10}O_{40}$ micellar catalyst.

3.2. CWAO properties of $[(C_nH_{2n+1})N(CH_3)_3]_{3+x}PV_xMo_{12-x}O_{40}$

3.2.1. Activity

A preliminary experiment was performed at 25 °C and atmospheric pressure in the existence of air and no catalysts (Fig. 2). No phenol degradation is detected, and the oxidation ability of O_2 at room temperature is limited without a catalyst. Fig. 2 shows the phenol degradation efficiency using different catalysts. Using CTAB as a catalyst, the degradation effect reaches a maximum value of 12.2% for about 30 min, which could be attributed to the adsorption effect, since no intermediates and CO_2 formed. From Fig. 2, the strength of the catalytic activity is arranged as follows: $(C_{16}TA)_4PVMo_{11}O_{40} < (C_{16}TA)_5PV_2Mo_{10}O_{40} \sim (C_{16}TA)_6PV_3Mo_9O_{40}$. The highest activity is obtained when using $(C_{16}TA)_6PV_3Mo_9O_{40}$ or $(C_{16}TA)_5PV_2Mo_{10}O_{40}$, which exhibits 95.3% degradation efficiency for 0.72 mM phenol. The catalytic performance is supposed to correspond to the redox potential with respect to vanadium substitution. Cyclic voltammetry on molybdovanadophosphoric salts indicates that the first redox potentials for the VO_2^+/VO^{2+} couple in a water/dioxane mixture are 0.46, 0.47, and 0.48 V, corresponding to $PVMo_{11}O_{40}^{4-}$, $PV_2Mo_{10}O_{40}^{5-}$, and $PV_3Mo_9O_{40}^{6-}$, respectively. This result shows that the substitution of Mo^{6+} with V^{5+} would lead to the generation of more reactive lattice oxygen associated with the Mo–O–V species [40]. The first reversible redox peak corresponding to one-electron oxidants/reductants of VO_2^+/VO^{2+} is essential for the catalytic process using molecular oxygen as an oxidant. The redox potential of phenol is 0.4 V, which shows that phenol could be oxidized by O_2 under $[(C_nH_{2n+1})N(CH_3)_3]_{3+x}PV_xMo_{12-x}O_{40}$. The similar trend in catalyst activity was also reported in the literature on aerobic oxidation of tetrahydrothiophene using $H_{3+x}[PV_xMo_{12-x}O_{40}]$ catalysts [41]. In Fig. 2, $PV_3Mo_9O_{40}^{6-}$ exhibits a higher catalytic activity than

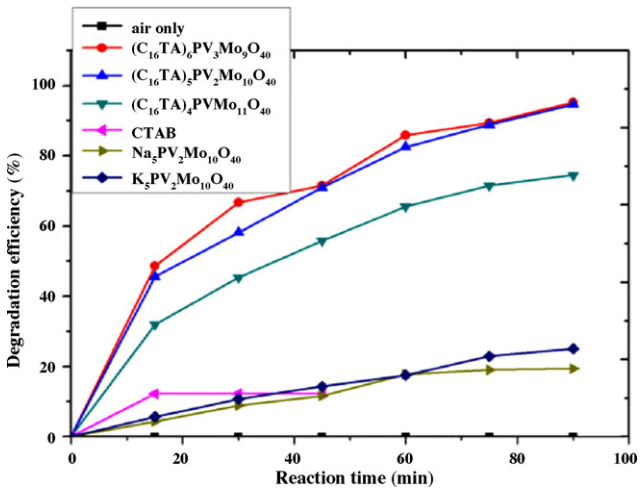

Fig. 2. Degradation efficiency of phenol by different $[(C_nH_{2n+1})N(CH_3)_3]_{3+x}PV_xMo_{12-x}O_{40}$ (0.92 mM) catalysts at room temperature, 100 mL of 0.72 mM phenol solution, with the air flowing rate 0.04 m^3/h.

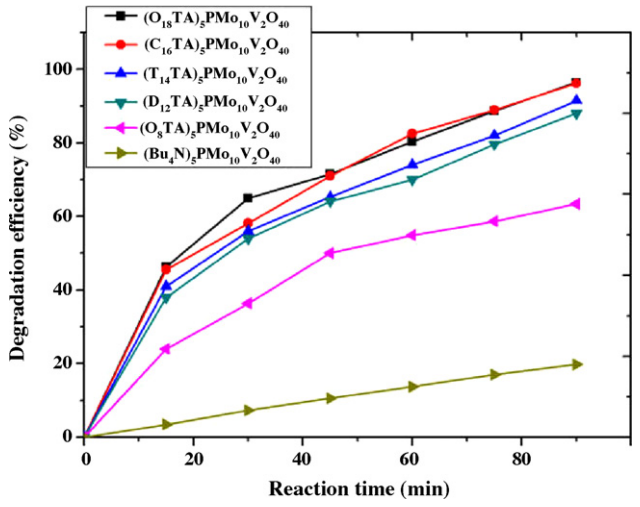

Fig. 3. Influence of length of chain of $[(C_nH_{2n+1})N(CH_3)_3]_5PV_2M_{10}O_{40}$ on degradation of phenol at room temperature, 100 mL of 0.72 mM phenol solution, with the air flowing rate 0.04 m^3/h.

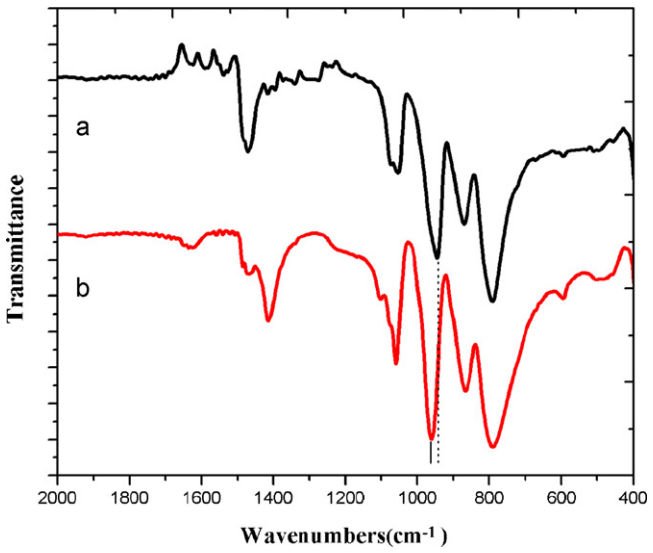

Fig. 4. The IR spectra of pure $(C_{16}TA)_5PV_2Mo_{10}O_{40}$ (a) and $(C_{16}TA)_5PV_2Mo_{10}O_{40}$ after adsorbing phenol (b).

$PV_2Mo_{10}O_{40}^{5-}$ in the beginning of the oxidation, but then the catalytic activity of the two catalysts tends to become equivalent. In the beginning, the difference of the two catalysts is visible. As reaction time increases, the effect of V becomes less obvious, and the degradation efficiency reaches its maximum.

Amphiphiles are molecules consisting of a hydrophilic head group and a hydrophobic (lipophilic) tail, which allow it to interact with both polar and nonpolar compounds. When the hydrophobic tail reaches a certain chain length, the amphiphiles reduce the unusually high surface tension of water to form micelles in water or media similar to water. Micelles are especially simple spherical supramolecules [25]. $[(C_nH_{2n+1})N(CH_3)_3]_{3+x}PV_xMo_{12-x}O_{40}$ contains a quaternary ammonium-hydrophobic tail and a POM hydrophilic head group, allowing it exhibit amphiphilic properties and to act as both catalyst and surfactant to assemble micelle in an aqueous solution.

The different length of quaternary ammonium cations of $[(C_nH_{2n+1})N(CH_3)_3]_5PV_2M_{10}O_{40}$ might lead to different catalytic performances (Fig. 3). $Na_5PV_2Mo_{10}O_{40}$ and $K_5PV_2Mo_{10}O_{40}$ – the soluble forms of POMs – show lower activity in phenol degradation, while degradation efficiency reaches 19.4% and 25.1%, respectively. As $Na_5PV_2Mo_{10}O_{40}$ and $K_5PV_2Mo_{10}O_{40}$ are homogeneous catalysts, the phenol molecules cannot assemble on their molecules. The hydrophobic chain of a surfactant must have a certain length (>C10) to enable successful micelle formation [25]. $(Bu_4N)_5PV_2Mo_{10}O_{40}$ with a shorter carbon chain less than C10 has difficulty in forming an micelle and only acts as heterogeneous catalyst, resulting in low degradation of phenol (19.7%). With the enhancement of the length from C8 to C18, the catalytic activity increases significantly from 63.4% for $(O_8TA)_5PV_2Mo_{10}O_{40}$ to 96.4% for $(O_{18}TA)_5PV_2Mo_{10}O_{40}$, respectively. The catalytic difference between $(C_{16}TA)_5PV_2Mo_{10}O_{40}$ (94.6%) and $(O_{18}TA)_5PV_2Mo_{10}O_{40}$ is less. This result confirms that the length of the carbolic chain of cations plays an important role in phenol oxidation. The surfactant-POMs act as both a catalyst and a surfactant to assemble micelles in water.

The high activity of micellar POM catalysts is attributed to the accumulation of phenol on the part of $PV_2Mo_{10}O_{40}$. It had been reported that organic molecules with aromatic ring can firstly assemble on the surface of the micelles by hydrogen bond formation between water molecules outside of micelles and π electron interaction [42]. And aromatic compounds are often found to be present in both the head-group region and the core [25].

The IR spectra of $(C_{16}TA)_5PV_2Mo_{10}O_{40}$ and its adsorbed phenol confirm the assembly of phenol on POM head region (Fig. 4). The spectrum of $(C_{16}TA)_5PV_2Mo_{10}O_{40}$ adsorbed phenol gives the four characteristic peaks at 1059 cm^{-1} (νas P–O_a, internal oxygen connecting P and Mo), 960 cm^{-1} (νas Mo–O_d, terminal oxygen bonding to Mo atom), 866 cm^{-1} (νas Mo–O_b, edge-sharing oxygen connecting Mo), 791 cm^{-1} (νas Mo–O_c, corner-sharing oxygen connecting Mo_3O_{13} units) corresponding to $[PV_2Mo_{10}O_{40}]^{5-}$ structural vibrations. The Mo–O_d vibration band shifts to higher frequency (960 cm^{-1}), indicating that some interaction occurs between the OH group from phenol and the terminal oxygen atom from the POM molecules. Therefore, reactant phenol is accumulated compared to the surrounding water phase through interactions with the micelle surface or through insertion into the micelle itself. This leads to an increase in reaction rate (Scheme 1).

Phenol adsorption on catalysts also confirms the accumulation of phenol on the micellar POM system (Fig. 5). Nitrogen was passed over a phenol solution (C_0 = 0.72 mM, 100 mL) in the presence of catalysts to ensure that O_2 does not enter into the experimental system. Phenol adsorption on $(C_{16}TA)_5PV_2Mo_{10}O_{40}$ reaches saturation after 15 min. Compared to the adsorption of CTAB (Fig. 2), $(C_{16}TA)_5PV_2Mo_{10}O_{40}$ can enhance phenol adsorption on micelles. This result is attributed to the interaction between the OH group of phenol and the terminal oxygen atom from POM. In addition, an increase in the length of quaternary ammonium cations can increase the adsorption effect. The adsorption effects of C8 and C18 are only 14.4% and 20%, respectively, which can be attributed to enhanced lipophilicity. The amphiphilic quaternary ammonium

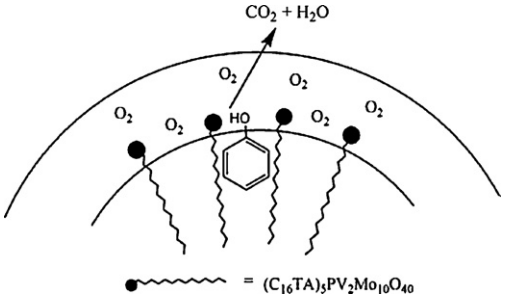

Scheme 1. Schematic representation of orientation of reactants in a micellar POM catalyst and phenol being oxidized by O_2 to CO_2.

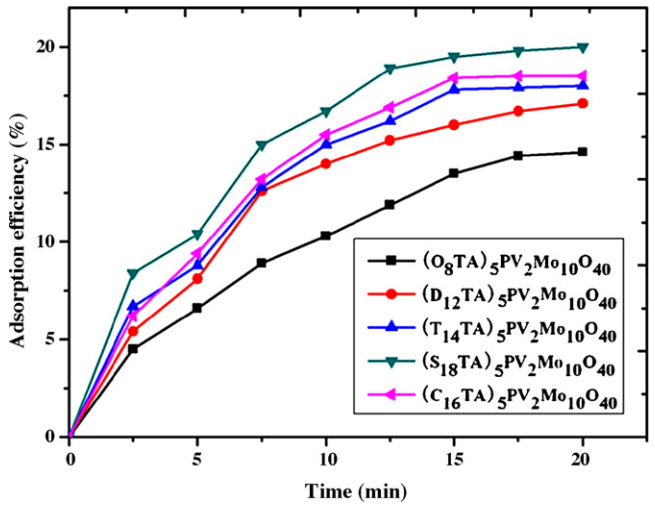

Fig. 5. The adsorption of phenol on catalysts $[(C_nH_{2n+1})N(CH_3)_3]_5PV_2M_{10}O_{40}$ at room temperature.

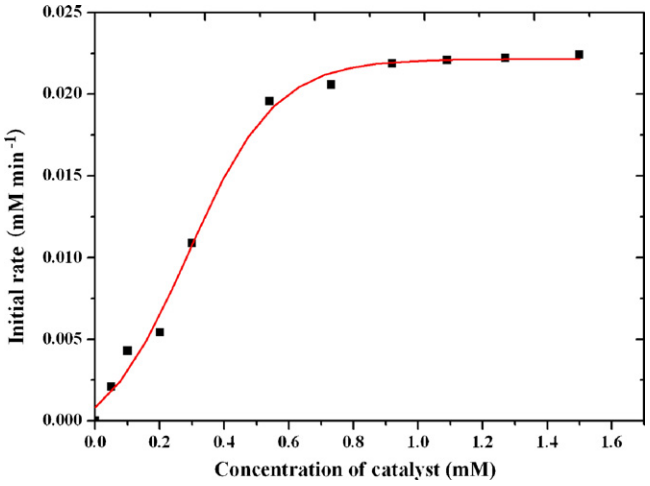

Fig. 7. Initial rate vs. the concentration of $(C_{16}TA)_5PV_2Mo_{10}O_{40}$ in degradation of phenol in 100 mL of 0.72 mM phenol solution with the air flowing rate 0.04 m^3/h at room temperature. The initial rate is based on the degradation after 15 min.

with the longest chain generally exhibits more lipophilicity than the shorter chains. Therefore, phenol adsorption on a micellar POM system can be increased with an increase in length.

The solution pH has a significant influence on the oxidation efficiency of phenol (Fig. 6). Fig. 6 shows the degradation efficiency of phenol over $(C_{16}TA)_5PV_2Mo_{10}O_{40}$ at pH values of 1.7, 2.5, 3.0, 4.0, 5.0, 6.0, and 7.0. The catalysts did not dissolve into the reaction mixture at these pH values. Phenol degradation decreases from 94.6% to 84.7% as pH values increase from 1.7 to 7.0. An increase in pH leads to the ionization of phenol to form Ph–O$^-$. The surface charges of POMs are negative, so these repel phenol molecules, resulting in a decrease in phenol adsorption onto the catalyst and a decrease in degradation efficiency.

The influence of $(C_{16}TA)_5PV_2Mo_{10}O_{40}$ on phenol degradation is presented in Fig. 7. The initial rate shows an increasing trend as the concentration of $(C_{16}TA)_5PV_2Mo_{10}O_{40}$ increases. A reaction rate plateau appears when the $(C_{16}TA)_5PV_2Mo_{10}O_{40}$ concentration exceeds 0.92 mM. This catalysis observed under the experimental conditions is in agreement with similar bimolecular reactions [43].

To study the effect of the amount of phenol, experiments were performed using different concentrations (0.72, 1.44, 2.16, 2.88, 3.6, 4.32, and 5.4 mM), while other variables were kept constant (Fig. 8). The rate of degradation decreases when the phenol concentration increases, indicating that phenol degradation depends on its initial concentration. This phenomenon may be due to the decrease of catalytic active sites. Increasing the initial concentration of phenol leads to more phenol molecules absorbed on the catalyst. Thus, an increase in the amount of substrates accommodating the catalyst inhibits the action of the catalyst with O_2. In this way, the degradation efficiency is decreased.

Fig. 9 shows the trend of phenol conversion with temperature and reaction time. The catalytic activity of $(C_{16}TA)_5PV_2Mo_{10}O_{40}$ at lower temperatures, such as 273 K, is presented. Temperature has a significant effect on phenol degradation. The catalytic activity of $(C_{16}TA)_5PV_2Mo_{10}O_{40}$ is high even at a lower temperature, where the degradation efficiency is 81.6% for a 90 min reaction. With an increase in temperature, degradation efficiency increases significantly, and phenol conversion reaches 97.4% at 303 K. Therefore, higher temperatures can considerably promote phenol degradation.

3.2.2. Mineralization

To further evaluate the oxidation ability of micellar POM catalysts toward phenol, mineralization was studied by monitoring TOC changes in reaction systems. The TOC reductions

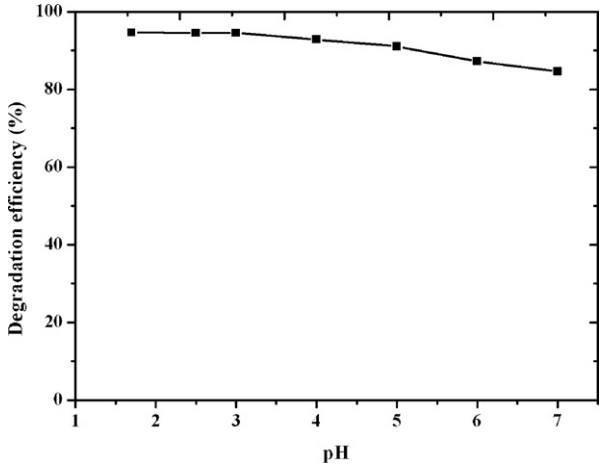

Fig. 6. The degradation efficiency of phenol on catalysts $[(C_nH_{2n+1})N(CH_3)_3]_5PV_2M_{10}O_{40}$ at room temperature at different pH values for 90 min.

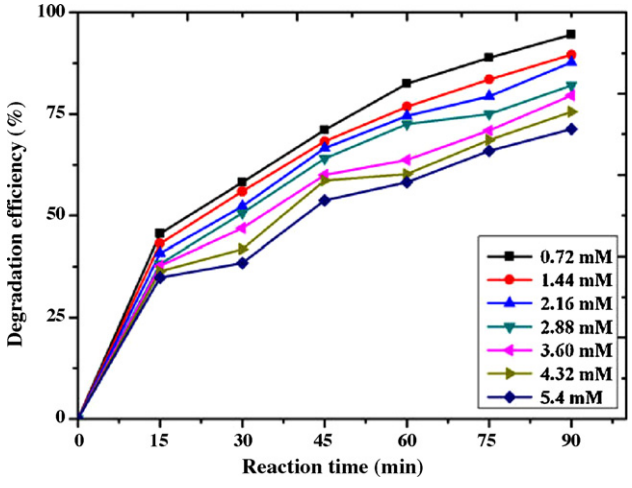

Fig. 8. The effect of substrate concentrations on degradation of phenol by $(C_{16}TA)_5PV_2Mo_{10}O_{40}$ (0.92 mM) with the air flowing rate 0.04 m^3/h at room temperature for 90 min.

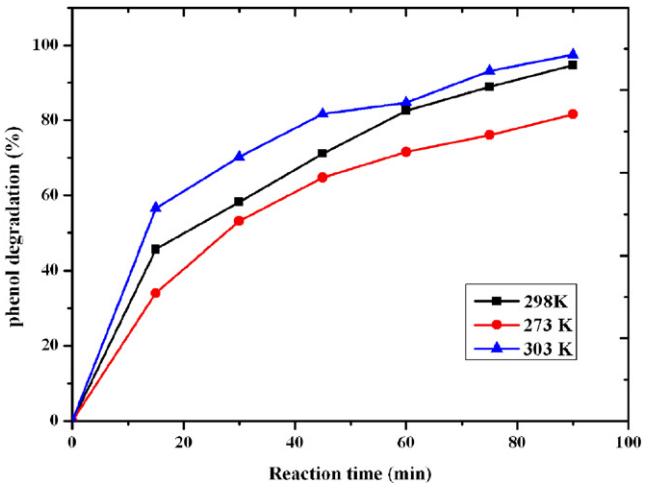

Fig. 9. The influence of reaction temperature on the degradation of phenol by $(C_{16}TA)_5PV_2Mo_{10}O_{40}$ (0.92 mM) in 100 mL of 0.72 mM phenol solution with the air flowing rate 0.04 m^3/h for 90 min.

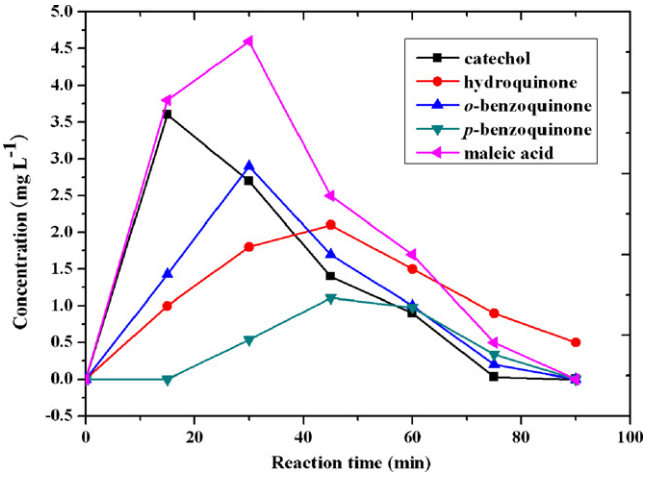

Fig. 11. Evolution of hydroquinone, catechol, and then p-benzoquinone, o-benzoquinone, and maleric acid in the solution during CWAO degradation of phenol with $(C_{16}TA)_5PV_2Mo_{10}O_{40}$ (0.92 mM) in 100 mL of 0.72 mM phenol solution with the air flowing rate 0.04 m^3/h for 90 min at room conditions.

of phenol over $(C_{16}TA)_4PVMo_{11}O_{40}$, $(C_{16}TA)_5PV_2Mo_{10}O_{40}$, and $(C_{16}TA)_6PV_3Mo_9O_{40}$ reach 67.8%, 91.4%, and 93.0%, respectively, at about 90 min.

The COD reflects the extent of contamination by the reductive substances in water. A significant decrease in COD is observed. The COD removal efficiencies over $(C_{16}TA)_4PVMo_{11}O_{40}$, $(C_{16}TA)_5PV_2Mo_{10}O_{40}$, and $(C_{16}TA)_6PV_3Mo_9O_{40}$ are about 70.8%, 97.6%, and 98.5%, respectively, at about 90 min.

3.2.3. Mechanism

Depending on the nature and redox properties of the substrate, electron-transfer, O-transfer, and radical pathways have been suggested in the oxidation of organic substrates using POMs as catalysts. Generally, organic degradation by WAO is recognized as a free radical mechanism. Hydroxyl radical (OH•), an extremely high-potential oxidizing agent with a short life, can oxidize organic substrates and generate other free radicals [36]. To determine the main active species responsible for the degradation of phenol molecules, a comparative study was undertaken for the scavenger-loaded condition (Fig. 10). The formation of possible oxidative intermediate species, such as singlet oxygen ($^1O_2$), superoxide ($O_2^{\bullet -}$), and hydroperoxy ($HO_2^{\bullet}$), or (OH•), under CWAO conditions was investigated indirectly with the use of appropriate quenchers for these species. In this type of experiment, a comparison was made between the original degradation curves of phenol/$(C_{16}TA)_5PV_2Mo_{10}O_4$ dispersions and those obtained after the addition of millimolar concentrations of quenchers in the initial solution under otherwise identical conditions. In Fig. 10, Curve a is the degradation curve without any quenchers, and Curves b, c, and d represent the addition of KI (a quencher of OH• radical on catalyst surface [44]), sodium azide (NaN_3, a singlet oxygen quencher [45] but may also interact with OH• radical [46]), and p-benzoquinone ($C_6H_4O_2$, BQ, a quencher of superoxide radical [47]), respectively. Both NaN_3 and KI affect the degradation rate of phenol throughout the experiment, indicating that the active oxidative species involved in this CWAO system is either $^1O_2$ or OH•. The effect of NaN_3 is higher than that of KI, showing that, besides OH•, single oxygen $^1O_2$ was formed as a possible oxidative intermediate species during the reaction. BQ does not affect the degradation rate of phenol, showing that $O_2^{\bullet -}$ was not the oxidative intermediate species. These results demonstrate that the reaction takes place through a radical and single oxygen mechanism. These can help elucidate the mechanism of CWAO degradation of phenol over the $(C_{16}TA)_5PV_2Mo_{10}O_4$ catalyst.

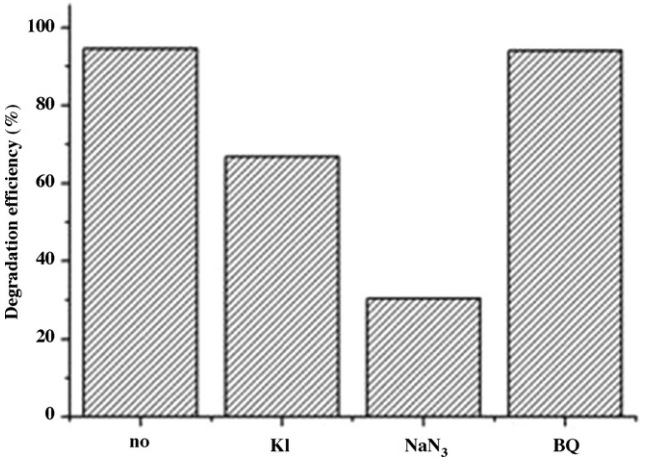

Fig. 10. Effects of scavenging agents on degradation of phenol in the presence of 2 mM of 1,4-benzoquinone (BQ), NaN_3 and KI with $(C_{16}TA)_5PV_2Mo_{10}O_{40}$ (0.92 mM) in 100 mL of 0.72 mM phenol solution with the air flowing rate 0.04 m^3/h for 90 min at room conditions.

In addition, the mechanism of CWAO degradation of phenol is proposed over $(C_{16}TA)_5PV_2Mo_{10}O_4$ catalyst.

At first, the reactants (phenol and dioxygen) reached the surface and were adsorbed on the surface by a hydrogen bonding interaction between hydroxyl groups from phenol and O atom from POMs. Then phenol molecules were accessible to the active sites anchored within micellar particles (Scheme 1). This adsorption reached equilibrium after the suspension was stirred for 15 min.

Second, the catalysts are reduced by phenol RH to generate R• radical and the reduced form of POM_{red}. Next, •OH can be formed by a free radical chain auto-oxidation process in the presence of O_2, so that the organic molecules can be degraded by the •OH radical to initiate phenol degradation. Phenol is oxidized first into hydroquinone and catechol and then into p-benzoquinone, o-benzoquinone, and maleric acid. The intermediates disappear as they are further oxidized into CO_2 and water (Fig. 11). Finally, the catalytic cycle is completed by the reoxidation of POM_{red} to POM_{ox} form using O_2 (Scheme 2).

In the end, the catalytic cycle is completed by reoxidation of POM_{red} by molecular oxygen to POM_{ox} form.

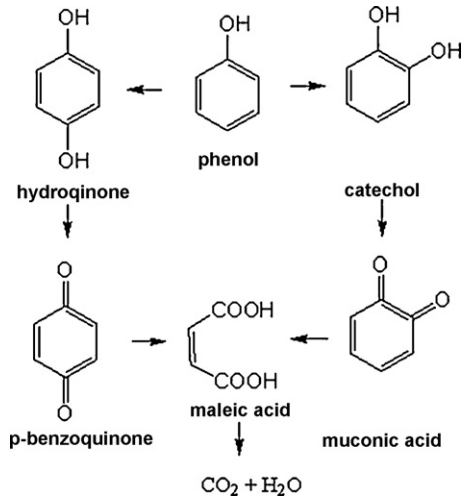

Scheme 2. Simplified procedure for phenol oxidation.

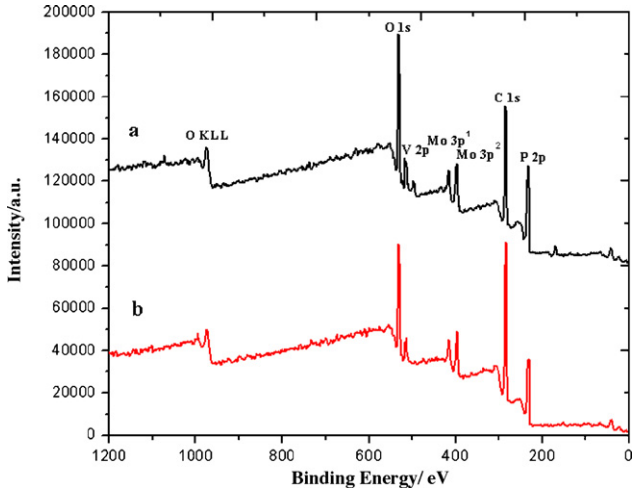

Fig. 12. Survey XPS spectra of $(C_{16}TA)_5PV_2Mo_{10}O_{40}$ catalyst before (a) and after the reaction (b).

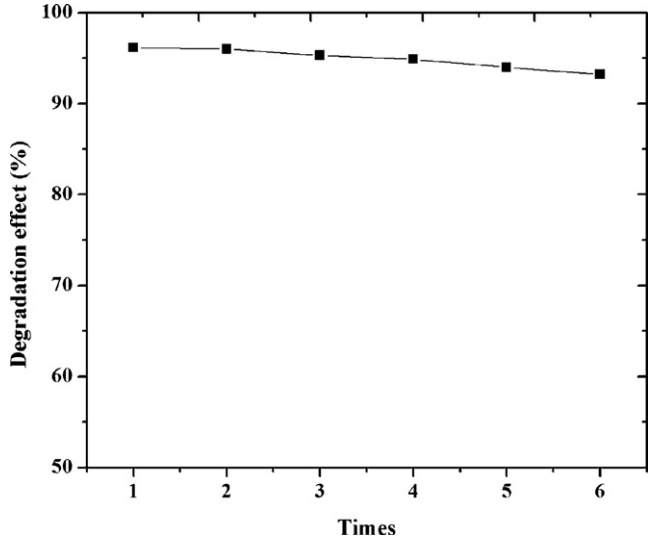

Fig. 13. Cycling runs in the degradation of phenol (100 mL of 0.72 mM phenol solution) in the presence of $(C_{16}TA)_5PV_2Mo_{10}O_{40}$ (0.92 mM) at room temperature with the air flowing rate 0.04 m^3/h.

3.2.4. Separation and recovery of the catalyst

The life span of a catalyst is a more important parameter for its evaluation. The regeneration of $(C_{16}TA)_5PV_2Mo_{10}O_{40}$ is of practical and economic importance. It can be easily achieved by the centrifugation of the yellow species from the reaction system. This residue was washed by water to produce pure $(C_{16}TA)_5PV_2Mo_{10}O_{40}$. The regenerated reagent is as reactive as the freshly prepared catalyst. Based on XPS analysis, the catalyst structure does not change after six repeated experiments (Fig. 12). Compared with the fresh catalyst (Fig. 12a), the bonding energies of Mo 3p, V 2p, and P 2p do not shift after the reaction (Fig. 12b). Because the oxidation states of Mo, P, and V do not change, the catalyst is deemed stable during the reaction, and the phenol molecules adsorbed on its surface can be easily removed by simple washing with water. The XPS also confirms the existence of a $(C_{16}TA)_5PV_2Mo_{10}O_{40}$ component, but bromine is not detected. The catalytic activity of phenol degradation is maintained efficiently after six repeated experiments, showing only a slight decrease in activity (Fig. 13). Moreover, the total amount of $(C_{16}TA)_5PV_2Mo_{10}O_{40}$ leaching through six runs of the reaction reaches only 5.1% of the starting amount.

4. Conclusion

A present study reported the synthesis of micellar POM system $[(C_nH_{2n+1})N(CH_3)_3]_{3+x}PV_xMo_{12-x}O_{40}$ ($x = 1, 2, 3$; $n = 8, 12, 14, 16, 18$) and employment as catalysts for CWAO of phenol at mild conditions. When treating phenol, $[C_{16}H_{33}N(CH_3)_3]_6PV_3Mo_9O_{40}$ exhibits an excellent activity under ambient conditions, while phenol molecules are completely mineralized into CO_2 within 90 min. The higher catalytic activity of micellar POM catalysts comes from the micellar structure and enrichment of phenol on catalysts, which can provide more chance for phenol reacting with O_2. Moreover, these catalysts are insoluble in water and stable during six reused times simply washed with water. This catalytic process is a commercial and green chemical pathway which exhibits potential industrial application in phenol degradation.

Acknowledgements

Supported by the National Natural Science Foundation of China (No. 20871026), Analysis and Testing Foundation of Northeast Normal University.

References

[1] F.J. Zimmerman, Wet air oxidation of hazardous organics in wastewater, US Patent 2 665 249 (1950).
[2] S.K. Bhargava, J. Tardio, J. Prasad, K. Föger, D.B. Akolekar, S.C. Grocott, Ind. Eng. Chem. Res. 45 (2006) 1221–1258.
[3] J. Levec, A. Pintar, Catal. Today 24 (1995) 51–58.
[4] F. Luck, Catal. Today 53 (1999) 81–91.
[5] F. Luck, Catal. Today 27 (1996) 195–202.
[6] L. Oliviero, J. Barbier Jr., S. Labruquère, D. Duprez, Catal. Lett. 60 (1999) 15–19.
[7] J. Barbier Jr., F. Delanoë, F. Jabouille, D. Duprez, G. Blanchard, P. Isnard, J. Catal. 177 (1998) 378–385.
[8] J. Levec, A. Pintar, Catal. Today 124 (2007) 172–184.
[9] A. Santos, P. Yustos, A. Quintanilla, S. Rodríguez, F. García-Ochoa, Appl. Catal. B: Environ. 39 (2002) 97–113.
[10] J. Wang, W. Zhu, S. Yang, W. Wang, Y. Zhou, Appl. Catal. B: Environ. 78 (2008) 30–37.
[11] C. Resini, F. Catania, S. Berardinelli, O. Paladino, G. Busca, Appl. Catal. B: Environ. 84 (2008) 678–683.
[12] A. Eftaxias, J. Font, A. Fortuny, J. Giralt, A. Fabregat, F. Stüber, Appl. Catal. B: Environ. 33 (2001) 175–190.
[13] A. Santos, P. Yustos, S. Gomis, G. Ruiz, F. García-Ochoa, Chem. Eng. Sci. 61 (2006) 2457–2467.
[14] H. Chen, A. Sayari, A. Adnot, F. Larachi, Appl. Catal. B: Environ. 32 (2001) 195–204.
[15] M. Stoyanova, S. Christoskova, M. Georgieva, Appl. Catal. A 249 (2003) 295–302.
[16] A. Cybulski, J. Trawczynski, Appl. Catal. B: Environ. 47 (2004) 1–13.
[17] L. Oliviero, J. Barbier Jr., D. Duprez, Appl. Catal. B: Environ. 35 (2001) 1–12.
[18] J. Barbier Jr., L. Oliviero, B. Renard, D. Duprez, Catal. Today 75 (2002) 29–34.

[19] J.C. Beziat, M. Besson, P. Gallzot, S. Durecuf, J. Catal. 182 (1999) 129–135.
[20] N. Mizuno, M. Misono, Chem. Rev. 98 (1998) 199–218.
[21] R. Neumann, A.M. Khenkin, Chem. Commun. (2006) 2529–2538.
[22] I.V. Kozhevnikov, Chem. Rev. 98 (1998) 171–198.
[23] T. Ressler, O. Timpe, F. Girgsdies, J. Wienold, T. Neisius, J. Catal. 231 (2005) 279–291.
[24] M.J. Birchmeier, C.G. Hill Jr., C.J. Houtman, R.H. Atalla, I.A. Weinstock, Ind. Eng. Chem. Res. 39 (2000) 55–64.
[25] T. Dwars, E. Paetzold, G. Oehme, Angew. Chem., Int. Ed. 44 (2005) 7174–7199.
[26] A. Witek, A. Koltuniewicz, B. Kurczewski, M. Radziejowska, M. Hatalski, Desalination 191 (2006) 111–116.
[27] A. Lambert, P. Plucinski, I.V. Kozhevnikov, Chem. Commun. 6 (2003) 714–715.
[28] J. Kaur, I.V. Kozhevnikov, Catal. Commun. 5 (2004) 709–713.
[29] R. Neumann, A.M. Khenkin, J. Org. Chem. 59 (1994) 7577–7579.
[30] H.Y. Lv, J.B. Gao, Z.X. Jiang, F. Jing, Y.X. Yang, G. Wang, C. Li, J. Catal. 239 (2006) 369–375.
[31] C. Li, Z.X. Jiang, J.B. Gao, Y.X. Yang, S.J. Wang, F.P. Tian, F.X. Sun, X.P. Sun, P.L. Ying, C.R. Han, Chem. Eur. J. 10 (2004) 2277–2280.
[32] M.L. Guo, Green Chem. 6 (2004) 271–273.
[33] H.Y. Lü, J.B. Gao, Z.X. Jiang, Y.X. Yang, B. Song, C. Li, Chem. Commun. (2007) 150–152.
[34] F. Chai, L.J. Wang, L.L. Xu, X.H. Wang, J.G. Huang, Dyes Pigments 76 (2008) 113–117.
[35] Y. Zhang, D.L. Li, Y. Chen, X.H. Wang, S.T. Wang, Appl. Catal. B: Environ. 86 (2009) 182–189.
[36] I. Arslan-Alaton, J.L. Ferry, Dyes Pigments 54 (2002) 25–36.
[37] Y.H. Guo, C. Hu, Mol. J. Catal. A: Chem. 262 (2007) 136–148.
[38] G.A. Tsigdinos, C.J. Hallada, Inorg. Chem. 7 (1968) 437–441.
[39] P. Mukherjee, K.J. Mysels, Critical Micelle Concentrations of Aqueous Surfactant System, NSRDS-NBS, 1971, p. 36.
[40] M. Akimoto, H. Ikeda, A. Okabe, E. Echigoya, J. Catal. 89 (1984) 196–208.
[41] C.L. Hill, R.D. Gall, J. Mol. Catal. A: Chem. 114 (1996) 103–111.
[42] S. Suzuki, P.G. Green, R.E. Bumgarner, S. Dasgupta, W.A. Goddard III, G.A. Blake, Science 257 (1992) 942–945.
[43] J.E. Klijn, J.B.F.N. Engberts, Org. Biomol. Chem. 2 (2004) 1789–1799.
[44] C. Karunakaran, R. Dhanalakshmi, Solar Energy Mater. Solar Cells 92 (2008) 1315–1321.
[45] F. Wu, N.S. Deng, H.L. Hua, Chemosphere 41 (2000) 1233–1238.
[46] S.H. Yoon, J.H. Lee, Environ. Sci. Technol. 39 (2005) 9695–9701.
[47] C. Schweitzer, R. Schmidt, Chem. Rev. 103 (2003) 1685–1757.